Preprints of the 21st IFAC World Congress (Virtual)
Berlin, Germany, July 12-17, 2020

Affine Formation Maneuver Control of Event-triggered Multi-agent Systems ⋆

Junyi Yang, Hao Yu, Tongwen Chen

Department of Electrical and Computer Engineering, University of Alberta, Edmonton, AB, T6G 1H9, Canada
(e-mail: junyi7@ualberta.ca; hy10@ualberta.ca; tchen@ualberta.ca).

Abstract: An event-triggered affine formation maneuver control problem is studied in this work. The formations are invariant for any affine transformation. An event-triggered mechanism is proposed for the closed-loop system under which the controller updates and information broadcasting are generated only when it is necessary to maintain the system behavior. The practical convergence is guaranteed for the closed-loop system and Zeno behavior is excluded. Simulations are provided to verify the effectiveness of the method.

Keywords: Event-triggered control, multi-agent systems, affine formation, maneuver control

1. INTRODUCTION

Due to wide applications in monitoring and control, search and rescue, sensor networks, control and estimation of multi-agent systems (MASs) have become an active area of research since last decade (Olfati-Saber and Murray, 2004). Formation control, as one of the major areas, has drawn a lot of attention (Oh et al., 2015). Under the classical setup, the formation control can be classified into three kinds, namely, distance-based (Sun et al., 2016), bearing-based (Trinh et al., 2018; Zhao and Zelazo, 2015), and position-based (Wang et al., 2014). The formation structures are invariant for rotation and scaling for the first two kinds, and are fixed for the last one. In the classical setup, the formation structures typically have only one degree of freedom (DOF) at most and are usually determined in advance.

When the agents are maneuvering in an unknown or hostile environment, they need to respond to some unexpected situations. Thus, it is preferred that the formation structures are more flexible. This concern can be tackled by an affine formation method which has been proposed in Lin et al. (2015); Zhao (2018) recently. The formation under this newly studied method has $n+1$ DOF for an MAS in an n dimensional (nD) space. For example, in a 2D space, the formations of MASs are invariant for any affine transformation which can be obtained by a rotation, a scaling along two different axis, then another rotation, and ending with a translation (Lin et al., 2015). Referring to the topological graph of the MASs under the affine formation method, different from the spanning tree condition used in classical setups, an $(n+1)$-rooted condition is considered for the formation problem in an nD space. Under this assumption, the associated generalized Laplacian matrices have $n+1$ zero eigenvalues, with the eigenvectors determined by a nominal configuration. Thus, the dimension of its kernel space is $n+1$, which provides extra n DOF in the formation structure, rather than 1 as in classical Laplacian matrices.

In Lin et al. (2015), an affine formation problem is considered in a consensus sense, which means the MAS converges to an affine formation determined by the initial states, and no specific formation can be assigned. However, in some circumstances, it is preferred that the MAS can maneuver along some specific formations. Inspired by Zhao (2018) and Xu et al. (2018), an affine formation maneuver problem is considered in this work, where the MAS aims at achieving a specific formation structure spanned by the kernel space of the associated Laplacian matrices, and at the same time, tracking some reference trajectories.

Another concern in MASs is the limited onboard energy and communication resources. Thus, the scheduling of controller updates and data transmissions becomes a critical and practical issue. The scheduling can be done in a time-triggered or an event-triggered fashion. For the first kind, the sampling period is predetermined which should guarantee the system performance over a wide range of operating conditions, see Lemmon (2010). This fixed sampling period may be conservative resulting in unnecessary controller updates and data transmissions. In MASs, the control tasks are usually fulfilled by the communication among agents. Thus, high-frequency sampling might cause traffic congestion in the network and increase packet dropout, see Ding et al. (2017). Frequent updates and transmissions also cause extra energy consumption (Zhang et al., 2016), which might reduce the life span of agents. In the light of this concern, an event-triggered mechanism is considered in this work. The controller updates and data transmissions are generated sporadically, only when it is essential for maintaining the system performance. As a result, less communication and energy consumption are required, with some comparable system performance.

The exclusion of Zeno behavior, in the sense that infinite events happen in a finite time interval, is a critical and challenging problem. In Borgers and Heemels (2014),

⋆ This work was supported by NSERC, and an Alberta EDT Major Innovation Fund.

the authors have pointed out that many existing event-triggered mechanisms would exhibit Zeno behavior when there is disturbances. Under the event-triggered mechanism proposed in this work, each agent broadcasts its velocity to the neighbors when the velocity error exceeds a predetermined threshold, and then, its neighbors use this information to construct their respective control inputs. This discontinuous velocity information can be regarded as a source of disturbance in the MASs, which might lead to Zeno behavior. In this work, the exclusion of Zeno behavior is guaranteed by the assumption of an acyclic graph and proved by recursively applying an event-separation property.

Notations: Let $\mathbb{R}$ ($\mathbb{Z}$) be the set of real (integer) numbers. The Euclidian norm of a vector $x \in \mathbb{R}^n$ is denoted by $\|x\|$. The Euclidean induced matrix norm of $A \in \mathbb{R}^{n\times m}$ is denoted by $\|A\|$. The transpose of a matrix $A \in \mathbb{R}^{n\times m}$ is denoted by A^{T}. $\otimes$ stands for the Kronecker product for matrices. Denote a column vector with entries all equal to one by $\mathbf{1}$ with appropriate dimensions. Let I_n be the identity matrix with dimension n; if the context is clear, the subscript n might be omitted. Let $|\Omega|$ be the cardinality of the set Ω. For two sets $\Omega_1, \Omega_2 \in \mathbb{R}^n$, define $\Omega_1 \backslash \Omega_2 := \{x \in \mathbb{R}^n | x \in \Omega_1, x \notin \Omega_2\}$. diag$(\cdots)$ denotes a diagonal matrix. For a real number s, $\lceil s \rceil$ denotes the smallest integer larger than or equal to s.

2. PRELIMINARIES

The interaction network among agents is described by a *signed directed graph* $\mathcal{G} = (\mathcal{V}, \mathcal{E}, \mathcal{A})$, which is composed of a node set $\mathcal{V} = \{1, 2, ..., N\}$, an edge set $\mathcal{E} \subseteq \mathcal{V} \times \mathcal{V}$, and an adjacency matrix $\mathcal{A} = [a_{ij}] \in \mathbb{R}^{N\times N}$ of the signed weights of $\mathcal{G}$ with $a_{ij} \neq 0 \Leftrightarrow (j, i) \in \mathcal{E}$ and $a_{ij} = 0 \Leftrightarrow (j, i) \notin \mathcal{E}$. An edge from node j (labelled as tail) to node i (labelled as head) is represented by the pair $(j, i) \in \mathcal{E}$, and the node j denotes the *in-neighbor* of i while the converse is called *out-neighbor*. The edge (j, i) indicates node i can receive information from node j. Denote $\mathcal{N}_i$ as the set of in-neighbors of node i, that is, $\mathcal{N}_i := \{j \in \mathcal{V} | (j, i) \in \mathcal{E}\}$. It is assumed that there is no self-loop, i.e., $a_{ii} = 0$, and the graph is a fixed topology. In a directed graph $\mathcal{G}$, a *path* is an alternating sequence of nodes and edges where the nodes in the sequence are different. The Laplacian L of a signed graph $\mathcal{G}$ is defined as

$$L = \text{diag}\left(\sum_{k\in\mathcal{N}_1} a_{1k}, \sum_{k\in\mathcal{N}_2} a_{2k}, ..., \sum_{k\in\mathcal{N}_N} a_{Nk}\right) - \mathcal{A}.$$

Referring to Lin et al. (2015), some useful concepts are recalled. In a direct graph $\mathcal{G}$, a node i is *k-reachable* ($k \geq 2$) from a non-singleton set $\mathcal{U} \subset \mathcal{V}$ if there is a path from a node in $\mathcal{U}$ to the node i after deleting any $k-1$ nodes that are different from i, that is, there are k disjoint paths from $\mathcal{U}$ to i. A directed graph $\mathcal{G}$ is *k-rooted* if there is a subset of k nodes (labelled as roots), from which every other node is k-reachable. For a k-rooted graph $\mathcal{G} = (\mathcal{V}, \mathcal{E})$, its spanning *$k$-tree* rooted at $\mathcal{R} := \{r_1, r_2, \ldots, r_k\} \subset \mathcal{V}$ is a spanning subgraph $\mathcal{T} = (\mathcal{V}, \bar{\mathcal{E}})$ satisfying

(1) every node $r \in \mathcal{R}$ has no in-neighbor;
(2) every node $r \notin \mathcal{R}$ has k in-neighbors;
(3) every node $r \notin \mathcal{R}$ is k-reachable from $\mathcal{R}$.

A *configuration* in $\mathbb{R}^d$ of a node set $\mathcal{V}$ is defined by their coordinates in the Euclidean space $\mathbb{R}^d$, denoted as $p = [p_1^{\mathrm{T}}, p_2^{\mathrm{T}}, \ldots, p_N^{\mathrm{T}}]^{\mathrm{T}}$ with $p_i \in \mathbb{R}^d, i \in \mathcal{V}$. A *framework* or *formation* in $\mathbb{R}^d$ is a directed graph $\mathcal{G}$ with its node i mapped to p_i, denoted as $\mathcal{F} := (\mathcal{G}, p)$.

3. PROBLEM FORMULATION

Consider a group of N agents in $\mathbb{R}^d$ with single-integrator dynamics under a signed directed graph $\mathcal{G}$:

$$\dot{p}_i(t) = u_i(t), \qquad i \in \mathcal{V} = \{1, 2, \ldots, N\}, \tag{1}$$

where $p_i \in \mathbb{R}^d$ denotes the position of agent i and u_i is the control input. The initial condition of the configuration is given as $p(0) = p_0 \in \mathbb{R}^{Nd}$. Furthermore, assume that $d \geq 2$ and $N \geq d + 2$.

Denote the first $N_l < N$ agents as the leaders and the remaining $N_f = N - N_l$ agents as the followers, that is, the leaders' node subset is $\mathcal{V}_l := \{1, 2, \ldots, N_l\}$ while the followers' node subset is $\mathcal{V}_f := \mathcal{V} \backslash \mathcal{V}_l$. The position of leaders is given by $p_l := [p_1^{\mathrm{T}}, p_2^{\mathrm{T}}, \ldots, p_{N_l}^{\mathrm{T}}]^{\mathrm{T}}$ and that of followers is given by $p_f := [p_{N_l+1}^{\mathrm{T}}, p_{N_l+2}^{\mathrm{T}}, \ldots, p_N^{\mathrm{T}}]^{\mathrm{T}}$. Referring to Zhao (2018), it is assumed that each leader $i \in \mathcal{V}_l$ does not have access to the information from other agents and it can move based on some pre-specified desirable trajectory $p_i^*(t)$ which will be defined later. Let the desired trajectories for leaders be given by $p_l^* := [p_1^{*\mathrm{T}}, p_2^{*\mathrm{T}}, \ldots, p_{N_l}^{*\mathrm{T}}]^{\mathrm{T}}$.

The *nominal formation* associated with $\mathcal{G}$ is defined as $\mathcal{F}_r := (\mathcal{G}, r)$, and $r = [r_1^{\mathrm{T}}, r_2^{\mathrm{T}}, \ldots, r_N^{\mathrm{T}}]^{\mathrm{T}} =: [r_l^{\mathrm{T}}, r_f^{\mathrm{T}}]^{\mathrm{T}} \in \mathbb{R}^{Nd}$ is a constant *nominal configuration*. The *affine image* of the nominal configuration is given by

$$\mathcal{S}(r) := \{p \in \mathbb{R}^{Nd} | p = (I \otimes A)r + \mathbf{1} \otimes b, A \in \mathbb{R}^{d\times d}, b \in \mathbb{R}^d\}, \tag{2}$$

where each pair (A, b) denotes one affine transformation.

Definition 1. (Target Affine Formation). The time-varying target affine formation is expressed as $F^*(t) := (\mathcal{G}, p^*(t))$ with the target configuration

$$p^*(t) = [I \otimes A(t)]r + \mathbf{1} \otimes b(t), \tag{3}$$

where $A(t) \in \mathbb{R}^{d\times d}$ and $b(t) \in \mathbb{R}^d$ are continuous of t. By (2), we have $p^*(t) \subseteq \mathcal{S}(r)$ for all t.

Recall that the leaders' position $p_l(t)$ is assumed to be equal to the desired target configuration p_l^*, i.e., $p_l(t) = p_l^*(t)$. Hence, in this paper, we will study the following affine formation maneuver control problem.

Problem 1: Design event-triggered control protocols $u_i(t), i \in \mathcal{V}_f$, such that the position $p_f(t)$ of followers can track the target configuration $p_f^*(t) := [p_{N_l+1}^{*\mathrm{T}}, \ldots, p_N^{*\mathrm{T}}]^{\mathrm{T}}$ practically, i.e., there is a constant $\varepsilon > 0$ satisfying $\sup \lim_{t\to\infty} \left\| p_f^*(t) - p_f(t) \right\| < \varepsilon$.

4. EVENT TRIGGERED MECHANISMS

In this section, the event-triggered affine formation maneuver control protocol will be proposed following an emulation-based manner. First, a continuous-time control protocol is introduced to ensure asymptotic tracking of the target formation. Then it will be transformed into an event-triggered one.

Initially, we introduce the following lemma on affine localizability. For a given point set $\{q_i\}_{i=1}^N$ in $\mathbb{R}^d$, the affine span $\mathcal{I}$ is defined as

$$\mathcal{I} := \left\{ \sum_{i=1}^N c_i q_i | c_i \in \mathbb{R}, \sum_{i=1}^N c_i = 1 \right\}.$$

Lemma 2. (Xu et al. (2018)). Suppose that

I) the nominal configuration r satisfies that $\{r_i\}_{i=1}^N$ has d-dimensional affine span;
II) the directed graph $\mathcal{G}$ is $(d+1)$-rooted and the leader set $\mathcal{V}_l$ is a root set.

Then, the nominal formation is affinely localizable, that is,

1) for any $p \in \mathcal{S}(r)$, p_f can be determined by p_l uniquely;
2) there exists a set of weights $a_{ij}, i, j \in \mathcal{V}$, associated with $\mathcal{G}$ such that the corresponding signed Laplacian $L \in \mathbb{R}^{N\times N}$ satisfies $(L \otimes I)p = 0$.

In the rest of this paper, we always assume the conditions of Lemma 2 are satisfied and the weights are selected based on Item 2). Then, the associated signed Laplacian can be expressed as

$$L = \left[\begin{array}{c|c} 0_{ll}^{(d+1)\times(d+1)} & 0_{lf}^{(d+1)\times(n-d-1)} \\ \hline L_{fl}^{(n-d-1)\times(d+1)} & L_{ff}^{(n-d-1)\times(n-d-1)} \end{array} \right]. \quad (4)$$

By using Lemma 2, one has that $\bar{L}_{ff}$ is nonsingular, and

$$\bar{L}_{fl} p_l^*(t) + \bar{L}_{ff} p_f^*(t) = 0, \quad (5)$$

where $\bar{L}_{fl} = L_{fl} \otimes I_d$ and $\bar{L}_{ff} = L_{ff} \otimes I_d$.

Lemma 3. (Xu et al. (2018)). Under the following continuous control protocols:

$$u_i(t) = -\frac{1}{L_{ii}} \sum_{j\in\mathcal{N}_i} a_{ij}[p_i(t) - p_j(t) - \dot{p}_j(t)], \quad (6)$$

where $L_{ii} \neq 0$ is the (i,i)-element of Laplacian L, the tracking error $\delta_f(t) := p_f(t) - \bar{L}_{ff}^{-1}\bar{L}_{fl}p_l^*(t)$ of followers converges globally and exponentially to zero.

Remark 1: Neighbors' inputs are required in controller (6). Such controllers have also been reported in Ren and Beard (2008), and Zheng and Wang (2012), where the leader's trajectory was unpredictable. In addition, by introducing an acyclic graph in Section 5, the contradiction in broadcasting input information between a pair of agents is excluded.

To avoid continuous network occupation and control updates, in the following, an event-triggered implementation of the controller in (6) is now discussed. Notice that there are two different parts in (6), namely, the (combined) relative position information $y_i(t) := \sum_{j\in\mathcal{N}_i} a_{ij}[p_i(t) - p_j(t)]$ and the in-neighbor's absolute velocity information $\dot{p}_j(t), j \in \mathcal{N}_i$. For these two kinds of information, different event-triggered mechanisms are designed as follows.

Since $y_i(t)$ can be deemed as local information (see, e.g., Zhang and Wang (2018)), agent i is able to measure it continuously. At each triggering instant $t_{k_i}^i$ for $k_i \in \mathbb{Z}_{\geq 0}$ and $i \in \mathcal{V}_f$, the relative position information will be sent to the local controller to update the control signal u_i. The triggering condition is given as

$$\|\epsilon_i(t)\|^2 \leq \sigma_1, i \in \mathcal{V}_f, \quad (7)$$

where $\sigma_1 > 0$ is a threshold constant, and the measurement error $\epsilon_i(t) := \hat{y}_i(t) - y_i(t), t \geq 0$, with $\hat{y}_i(t) = y_i(t_{k_i}^i), t \in [t_{k_i}^i, t_{k_i+1}^i)$.

The velocity information $\dot{p}_i(t), i \in \mathcal{V}$, is difficult to be continuously obtained by out-neighbors. Therefore, agent i will first measure its local velocity, then at each triggering instant $\tau_{k_i}^i, k_i \in \mathbb{Z}_{\geq 0}$, broadcast its own velocity information to its out-neighbors for their control updates. The triggering condition is

$$\|e_i(t)\|^2 \leq \sigma_2, i \in \mathcal{V}, \quad (8)$$

with a threshold constant $\sigma_2 > 0$, the broadcast error $e_i(t) := \hat{\dot{p}}_i(t) - \dot{p}_i(t), t \geq 0$, and $\hat{\dot{p}}_i(t) = \dot{p}_i(\tau_{k_i}^i), t \in [\tau_{k_i}^i, \tau_{k_i+1}^i)$.

During any two consecutive triggering instants, the controller will use the latest received signals to calculate the control signal. Thus, the event-triggered control protocols can be described by

$$\begin{aligned} u_i(t) &= -\frac{1}{L_{ii}}\hat{y}_i(t) + \frac{1}{L_{ii}} \sum_{j\in\mathcal{N}_i} a_{ij}\hat{\dot{p}}_j(t) \\ &= -\frac{1}{L_{ii}} \left[y_i(t) + \epsilon_i(t) - \sum_{j\in\mathcal{N}_i} a_{ij}(\dot{p}_j(t) + e_j(t)) \right], \end{aligned} \quad (9)$$

for $i \in \mathcal{V}_f$.

Due to the discontinuity of $\dot{p}_i(t), i \in \mathcal{V}_f$, under the event-triggered controller in (9), it is difficult to ensure a positive minimum inter-event time for the triggering condition in (8). Hence, we consider the following triggering performance called "separated events".

Problem 2: Show that the triggering conditions in (7-8) yield separated events. That is, for any given initial state $p_0 \in \mathbb{R}^{Nd}$, there exist constants $T_y \in (0,\infty)$ and $T_{\dot{p}} \in (0,\infty)$ satisfying, respectively,

$$\limsup_{t\to\infty} \frac{\left|\{t_{k_i}^i\}_{k_i=1}^\infty \cap [0,t]\right|}{t} < T_y \in (0,\infty), i \in \mathcal{V}_f,$$

and

$$\limsup_{t\to\infty} \frac{\left|\{\tau_{k_i}^i\}_{k_i=1}^\infty \cap [0,t]\right|}{t} < T_{\dot{p}} \in (0,\infty), i \in \mathcal{V}.$$

Remark 2: The event-separation property means that there are a finite number of triggering instants in any finite time interval, thus, it implies Zeno-freeness of the triggering time sequences. Moreover, it further ensures that the average triggering frequency can be upper bounded as the time goes to infinity. Note that if there is a positive lower bound for inter-event times, then the corresponding triggering sequence must be separated.

5. MAIN RESULTS

In this section, the main results will be given to solve Problems 1-2. First, the following theorem characterizes the tracking performance of the event-triggered controllers.

Theorem 4. The practical tracking property in Problem 1 can be ensured by the event-triggered controller in (9) and the triggering conditions in (7-8).

Proof. By substituting (9) into (1), one has for each follower $i \in \mathcal{V}_i$,

$$\dot{y}_i(t) = -y_i(t) - \epsilon_i(t) + \sum_{j\in\mathcal{N}_i} a_{ij} e_j(t). \tag{10}$$

Define $\epsilon(t) := [\epsilon_{d+2}^{\mathrm{T}}, \ldots, \epsilon_N^{\mathrm{T}}]^{\mathrm{T}}$, $e(t) := [e_1^{\mathrm{T}}, \ldots, e_N^{\mathrm{T}}]^{\mathrm{T}}$ and $w(t) = \bar{L}_{ff}\delta_f(t)$ with the tracking error δ_f given in Lemma 3. Then, (10) can be rewritten in the following compact form:

$$\dot{w}(t) = -w(t) - \epsilon(t) + \mathcal{A}_f e(t), \tag{11}$$

where $\mathcal{A}_f$ denotes the last $(n-d-1)$ rows of the adjacency matrix $\mathcal{A}$. According to the triggering conditions in (7-8), we have

$$\|\epsilon(t)\|^2 \le |\mathcal{V}_f|\,\sigma_1, \text{and, } \|\mathcal{A}_f e(t)\|^2 \le N\|\mathcal{A}_f\|^2\sigma_2.$$

Let $V(t) = \frac{1}{2}w^{\mathrm{T}}(t)w(t)$, then, its derivative along the solutions of (1) and (9) satisfies

$$\begin{aligned}\dot{V}(t) \le& -2V(t) + \|w(t)\|\,\|\epsilon(t)\| + \|w(t)\|\,\|\mathcal{A}_f e(t)\| \\ \le& -V(t) + |\mathcal{V}_f|\,\sigma_1 + N\|\mathcal{A}_f\|^2\sigma_2,\end{aligned}$$

which implies that the w-system is Lyapunov stable and

$$\sup \lim_{t\to\infty} V(t) \le 2(|\mathcal{V}_f|\,\sigma_1 + N\|\mathcal{A}_f\|^2\sigma_2) =: \frac{1}{2}\sigma_0^2.$$

The fact that $\bar{L}_{ff}$ is nonsingular further leads to

$$\sup \lim_{t\to\infty} \|\delta_f(t)\| \le \left\|\bar{L}_{ff}^{-1}\right\|\sigma_0, \tag{12}$$

and the proof is completed. □

To study the triggering performance, we introduce the following assumptions.

Assumption 1. For leaders $i \in \mathcal{V}_l$, its velocity $\dot{p}_i(t), t \in [0,\infty)$, is upper bounded by M_0.

Assumption 2. The graph $\mathcal{G}$ is an acyclic graph, i.e., there is no path that begins at a node $i \in \mathcal{V}$ and ends in one of the in-neighbors $j \in \mathcal{N}_i$.

For the events of relative position information, we can provide positive minimum inter-event times in the following theorem.

Theorem 5. For a given initial state p_0, the triggering instants generated by the triggering condition in (7) satisfy

$$\inf_{k_i\in\mathbb{Z}_{\ge 0}} (t_{k_i+1}^i - t_{k_i}^i) \ge T_0, i \in \mathcal{V}_f,$$

with some positive lower bound $T_0 > 0$.

Proof. By definitions, we have

$$y_f := \begin{bmatrix} y_{d+2} \\ \vdots \\ y_N \end{bmatrix} = \begin{bmatrix} \bar{L}_{fl} & \bar{L}_{ff} \end{bmatrix} \begin{bmatrix} p_l \\ p_f \end{bmatrix} = \bar{L}_{ff}\delta = w.$$

Thus, according to Theorem 4, for any given p_0, there is $M_1(p_0)$ such that $\|w(t)\| \le M_1, t \in \mathbb{R}_{\ge 0}$. Consequently,

$$\begin{aligned}\|\dot{y}_f(t)\| =& \|w(t) + \epsilon(t) - \mathcal{A}_f e(t)\| \\ \le& M_1 + \sqrt{|\mathcal{V}_f|\,\sigma_1} + \sqrt{N\|\mathcal{A}_f\|^2\sigma_2} \\ =:& \varphi_0.\end{aligned}$$

Since $\|\dot{y}_i(t)\| \le \|\dot{y}_f(t)\|$ and $\left\|\epsilon_i(t_{k_i}^i)\right\| = 0$ for all $i \in \mathcal{V}_f$ and $k_i \in \mathbb{Z}_{\ge 0}$, one can obtain that the inter-event times of the triggering condition in (7) are lower bounded by $\frac{\sqrt{\sigma_1}}{\varphi_0}$, and therefore, the proof is completed. □

For the analysis of the triggering conditions in (8), we introduce the following graph partition algorithm in Algorithm 1.

Algorithm 1 Partition of nodes in $\mathcal{G}$

1: Initial $m = 0$, $\mathcal{V}_0 := \mathcal{V}$, $\mathcal{E}_0 := \mathcal{E}$ and $\mathcal{G}_0 = \mathcal{G}(\mathcal{V}_0, \mathcal{E}_0)$;
2: Select all leaders as the 0th layer of agents, i.e., $\mathcal{L}_0 := \{i \in \mathcal{V}_l\}$ as the 0th layer;
3: **while** $\mathcal{V}_m \neq \mathcal{L}_m$
4: $m = m + 1$;
5: Generate a subgraph $\mathcal{G}_m(\mathcal{V}_m, \mathcal{E}_m)$ where
$$\mathcal{V}_m := \{i \in \mathcal{V} | i \notin \cup_{s=0}^{m-1}\mathcal{L}_s\},$$
$$\mathcal{E}_m := \{(i,j) \in \mathcal{E} | i,j \in \mathcal{V}_m\}.$$
6: Define the new mth layer of agents:
$$\mathcal{L}_m := \{i \in \mathcal{V}_m | \mathcal{N}_i \cap \mathcal{V}_m = \emptyset\}.$$
7: **end while**
8: **end**

Recall that both leaders and followers need to broadcast their velocity information. Thus, all nodes in the graph $\mathcal{G}$ are considered in the partition. In an acyclic directed graph, there always exists at least one node that does not have in-neighbors. Hence, the mth layer $\mathcal{L}_m$ contains all the agents without in-neighbors in the mth acyclic subgraph $\mathcal{G}_m$. Since there are a finite number of agents in the acyclic graph $\mathcal{G}$, Algorithm 1 must reach an end with finite layers, and denote the last layer as $q \in \mathbb{Z}_{\ge 1}$. An example is illustrated in Fig . 1. Furthermore, we have the following simple facts of the partition.

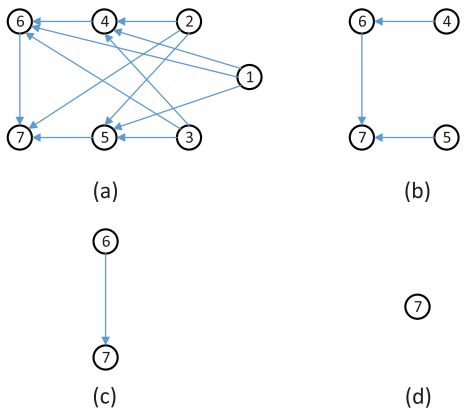

Fig. 1. An illustration of Algorithm 1. $\mathcal{G}_0(\mathcal{V}_0, \mathcal{E}_0)$ in (a) decides $\mathcal{L}_0 = \{1,2,3\}$; $\mathcal{G}_1(\mathcal{V}_1, \mathcal{E}_1)$ in (b) with $\mathcal{V}_1 = \{4,5,6,7\}$ yields $\mathcal{L}_1 = \{4,5\}$; $\mathcal{G}_2(\mathcal{V}_2, \mathcal{E}_2)$ in (c) with $\mathcal{V}_2 = \{6,7\}$ yields $\mathcal{L}_2 = \{6\}$; and finally $\mathcal{G}_3(\mathcal{V}_3, \mathcal{E}_3)$ in (d) with $\mathcal{V}_3 = \mathcal{L}_3 = \{7\}$ ends the algorithm.

Fact 1. For the layers of agents generated by Algorithm 1,

(1) $\mathcal{V} = \cup_{m=0}^{q}\mathcal{L}_m$;
(2) for any $m \in \{1,2,\ldots,q\}$, $\cup_{i\in\mathcal{L}_m}\mathcal{N}_i \subset \cup_{j=0}^{m-1}\mathcal{L}_j$.

Remark 3: The number of layers of an agent $i \in \mathcal{V}$ characterizes the "distance" between the agent and the roots (i.e., leader agents). For large-scale multi-agent systems, it is preferred to implement the communication topology with more layers due to some practical limitations, such as the spatial distribution or the broadcast ability of agents.

Based on the analysis above, we present the results of triggering sequences $\{\tau_{k_i}^i\}_{k_i=0}^{\infty}$ for $i \in \mathcal{V}$.

Theorem 6. Suppose that Assumptions 1-2 hold for the plant in (1) associated with the graph $\mathcal{G}$. For a given initial state p_0, the triggering condition in (8) generates separated events for all $i \in \mathcal{V}$.

Proof. First, for the leader $i \in \mathcal{L}_0 = \mathcal{V}_l$, the boundedness of $\dot{p}_i(t), t \in [0, \infty)$ guarantees a positive lower bound of inter-event times, which can be given as

$$\inf_{k_i \in \mathbb{Z}_{\geq 0}} (\tau_{k_i+1}^i - \tau_{k_i}^i) \geq \frac{\sqrt{\sigma_2}}{M_0}, i \in \mathcal{L}_0,$$

with M_0 defined in Assumption 1.

Assumption 2 ensures the feasibility of Algorithm 1; hence, we consider the agents in $\mathcal{L}_1 \subset \mathcal{V}_f$. According to the event-triggered controller in (9), for any $i \in \mathcal{V}_f$, the events from the triggering condition in (8) only occur when the relative position information of agent i or the absolute velocity information of its in-neighbors $j \in \mathcal{N}_i$ is updated, i.e., $\tau_{k_i}^i, k_i \in \mathbb{Z}_{\geq 0}$ belongs to $\{t_{k_i}^i\}_{k_i}^{\infty}$ or $\{\tau_{k_j}^j\}_{k_j=0}^{\infty}$ with $j \in \mathcal{N}_i$.

Based on Theorem 5 and Item (2) in Fact 1, one has, for any given interval $[a, b]$ with $a \geq b \geq 0$,

$$\left|[a,b] \cap \{t_{k_i}^i\}_{k_i}^{\infty}\right| < \left\lceil \frac{(b-a)\varphi_0}{\sqrt{\sigma_1}} \right\rceil + 1, i \in \mathcal{L}_1;$$

$$\left|[a,b] \cap \{\tau_{k_j}^j\}_{k_i}^{\infty}\right| < \left\lceil \frac{(b-a)M_0}{\sqrt{\sigma_2}} \right\rceil + 1, j \in \mathcal{N}_i, i \in \mathcal{L}_1.$$

Hence, it can be obtained that, for $i \in \mathcal{L}_1$,

$$\begin{aligned}\left|[a,b] \cap \{\tau_{k_i}^i\}_{k_i}^{\infty}\right| <& \chi_p(b-a) + \sum_{j \in \mathcal{L}_0 \cap \mathcal{N}_i} \chi_v^{0,j}(b-a) \\ =:& \chi_v^{1,i}(b-a),\end{aligned}$$

where $\chi_p(s) := \left\lceil \frac{s\varphi_0}{\sqrt{\sigma_1}} \right\rceil + 1$ and $\chi_v^{0,j}(s) := \left\lceil \frac{sM_0}{\sqrt{\sigma_2}} \right\rceil + 1, j \in \mathcal{L}_0$ for $s \geq 0$. The subscript "p" means position while "v" represents velocity. The superscript (l, i) stands for agent i in layer $\mathcal{L}_l$. Thus, the events for agent $i \in \mathcal{L}_1$ are separated. In detail, we have that for $i \in \mathcal{L}_1$,

$$\limsup_{t \to \infty} \frac{\left|\{\tau_{k_i}^i\}_{k_i=1}^{\infty} \cap [0,t]\right|}{t} < \frac{\varphi_0}{\sqrt{\sigma_1}} + |\mathcal{L}_0 \cap \mathcal{N}_i| \frac{M_0}{\sqrt{\sigma_2}}. \quad (13)$$

Suppose that the event-separation property holds for the agents in the layers $\{\mathcal{L}_0, \ldots, \mathcal{L}_m\}$ with $m \leq q-1$ and q being the total number of layers. Specifically, for any given $a \geq b \geq 0$,

$$\left|[a,b] \cap \{\tau_{k_i}^i\}_{k_i}^{\infty}\right| \leq \chi_v^{s,i}(b-a) \quad (14)$$

holds for all $i \in \mathcal{L}_s$ and $s \in \{1, \ldots, m\}$.

Now consider the agent $i \in \mathcal{L}_{m+1}$. From Theorem 5,

$$\left|[a,b] \cap \{t_{k_i}^i\}_{k_i}^{\infty}\right| < \chi_p(b-a), i \in \mathcal{L}_{m+1}. \quad (15)$$

Since $\mathcal{N}_i \subset \cup_{j=0}^m \mathcal{L}_j, i \in \mathcal{L}_{m+1}$ from Fact 1, combining (14-15) leads to

$$\begin{aligned}\left|[a,b] \cap \{\tau_{k_i}^i\}_{k_i}^{\infty}\right| <& \chi_p(b-a) + \sum_{t=0}^{m} \sum_{j \in \mathcal{L}_t \cap \mathcal{N}_i} \chi_v^{j,t}(b-a) \\ =:& \chi_v^{m+1,i}(b-a).\end{aligned} \quad (16)$$

By recursively applying (13) to (16), one can show that the events caused by the triggering condition in (8) of agent $i \in \mathcal{L}_{m+1}$ are separated. The analysis above can be extended to all the agents in the graph $\mathcal{G}$ due to Item (1) in Fact 1; and therefore, the proof is completed. □

Remark 4: According to Theorems 4-6, the triggering conditions in (7-8) provide a tradeoff between the tracking performance and the triggering performance. Smaller thresholds σ_1 and σ_2 could lead to higher tracking accuracy that is scaled by σ_0 in (12) but increases the number of events.

Remark 5: From the proof of Theorem 6, the events of an agent in a higher layer would be triggered more frequently than those in a lower layer. According to Remark 2, this property demonstrates the relationship between the system size and the communication load.

Remark 6: When there exists cycles in the graph, such as, between agents i and j, each of the agents can be regarded as the lower layer of the other one. In this case, a "positive feedback" effect on their events of absolute velocity information may happen. The events in agent i would promote the events in agent j, which could conversely accelerate the triggering of agent i. As a result, the events would not be separated as they are triggered faster and faster. How to design the event-triggered affine formation maneuver control for the systems containing cyclic topology will be left as future work.

6. SIMULATIONS

In this section, the effectiveness of the event-triggered control protocol is illustrated by simulations. The interaction network among agents is shown as in Fig. 1(a). The nominal formation r and the associated signed Laplacian are chosen the same as the ones used in Xu et al. (2018).

The thresholds for triggering conditions in (7) and (8) are chosen as $\sigma_1 = 0.05$ and $\sigma_2 = 0.1$, respectively. Fig. 2 shows the trajectories of the agents, where the practical time-varying affine formation maneuver is realized. Fig. 3 shows the tracking errors of the followers, with the steady-state errors given in Table 1. Here, δ_x and δ_y represent the tracking errors along x axis and y axis, respectively. The numbers of events are shown in Table 2. The agents in the higher layer are triggered more frequently than those in the lower layer, which coincides with the analysis in Remark 4. In addition, the tracking errors of the agents in the higher layer are larger than the ones in the lower layer. This is reasonable, since the control protocol relys on the information collected from the agents in the lower layers. The tracking errors are accumulated layer by layer.

Table 1. Steady-State Tracking Errors: with smaller thresholds

Agent	A_4	A_5	A_6	A_7
Steady-state error δ_x	0.6063	0.5925	1.4063	1.9263
Steady-state error δ_y	0.0131	0.0156	0.0126	-0.0731

Tables 3 and 4 show the steady-state errors and the numbers of events when the thresholds in (7) and (8) are chosen as $\sigma_1 = 0.1$ and $\sigma_2 = 0.2$, respectively. Large thresholds cause large tracking errors, however they reduce the frequency of controller updates and information broadcasting, which confirms the tradeoff explained in Remark 3.

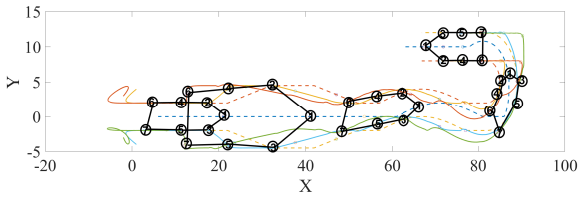

Fig. 2. Trajectories of the agents: Here, the dash lines represent the trajectories of the leaders, the solid lines represents the trajectories of the followers

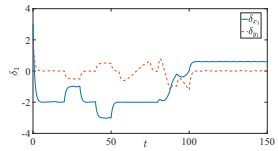

(a) Error of agent $4 \in \mathcal{L}_1$

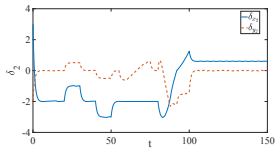

(b) Error of agent $5 \in \mathcal{L}_1$

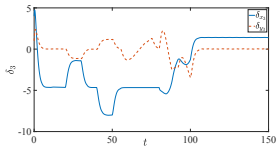

(c) Error of agent $6 \in \mathcal{L}_2$

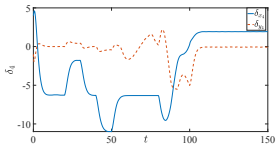

(d) Error of agent $7 \in \mathcal{L}_3$

Fig. 3. Tracking errors of the followers, with larger thresholds

Table 2. Number of Events: with smaller thresholds

Agent	A_4	A_5	A_6	A_7
Updates of relative position	373	424	943	1386
Broadcasting of velocity	168	182	333	342
Agent	A_1	A_2	A_3	
Broadcasting of velocity	44	29	49	

Table 3. Steady-State Tracking Errors: with larger thresholds

Agent	A_4	A_5	A_6	A_7
Steady-state error δ_x	0.8741	0.6908	2.0886	2.3037
Steady-state error δ_y	-0.0665	-0.0508	-0.2324	-0.2220

Table 4. Number of Events: with larger thresholds

Agent	A_4	A_5	A_6	A_7
Updates of relative position	209	225	529	755
Broadcasting of velocity	89	96	176	187
Agent	A_1	A_2	A_3	
Broadcasting of velocity	27	18	28	

7. CONCLUSIONS

An event-triggered affine formation maneuver problem was solved in this work. Under the proposed control protocol, the followers practically tracked the target configuration. In addition, Zeno behavior was excluded when the MAS was connected by an acyclic graph. The design of an event-triggered mechanism under the cyclic topology will be considered in the future study.

REFERENCES

D.P. Borgers and W.P.M.H. Heemels. Event-separation properties of event-triggered control systems. *IEEE Transactions on Automatic Control*, 59(10):2644–2656, 2014.

L. Ding, Q.L. Han, X. Ge, and X.M. Zhang. An overview of recent advances in event-triggered consensus of multiagent systems. *IEEE Transactions on Cybernetics*, 48 (4):1110–1123, 2017.

M.D. Lemmon. Event-triggered feedback in control, estimation, and optimization. In *Networked Control Systems*, pages 293–358. Springer, 2010.

Z. Lin, L. Wang, Z. Chen, M. Fu, and Z. Han. Necessary and sufficient graphical conditions for affine formation control. *IEEE Transactions on Automatic Control*, 61 (10):2877–2891, 2015.

K.K. Oh, M.C. Park, and H.S. Ahn. A survey of multi-agent formation control. *Automatica*, 53:424–440, 2015.

R. Olfati-Saber and R.M. Murray. Consensus problems in networks of agents with switching topology and time-delays. *IEEE Transactions on Automatic Control*, 49 (9):1520–1533, 2004.

W. Ren and R.W. Beard. Consensus algorithms for double-integrator dynamics. *Distributed Consensus in Multi-vehicle Cooperative Control: Theory and Applications*, pages 77–104, 2008.

Z. Sun, S. Mou, B.D.O. Anderson, and M. Cao. Exponential stability for formation control systems with generalized controllers: A unified approach. *Systems & Control Letters*, 93:50–57, 2016.

M.H. Trinh, S. Zhao, Z. Sun, D. Zelazo, B.D.O. Anderson, and H.S. Ahn. Bearing-based formation control of a group of agents with leader-first follower structure. *IEEE Transactions on Automatic Control*, 64(2):598–613, 2018.

W. Wang, J. Huang, C. Wen, and H. Fan. Distributed adaptive control for consensus tracking with application to formation control of nonholonomic mobile robots. *Automatica*, 50(4):1254–1263, 2014.

Y. Xu, S. Zhao, D. Luo, and Y. You. Affine formation maneuver control of multi-agent systems with directed interaction graphs. In *37th Chinese Control Conference (CCC)*, pages 4563–4568. IEEE, 2018.

X.M. Zhang, Q.L. Han, and B.L. Zhang. An overview and deep investigation on sampled-data-based event-triggered control and filtering for networked systems. *IEEE Transactions on Industrial Informatics*, 13(1):4–16, 2016.

Z. Zhang and L. Wang. Distributed integral-type event-triggered synchronization of multiagent systems. *International Journal of Robust and Nonlinear Control*, 28 (14):4175–4187, 2018.

S. Zhao. Affine formation maneuver control of multiagent systems. *IEEE Transactions on Automatic Control*, 63 (12):4140–4155, 2018.

S. Zhao and D. Zelazo. Translational and scaling formation maneuver control via a bearing-based approach. *IEEE Transactions on Control of Network Systems*, 4(3):429–438, 2015.

Y. Zheng and L. Wang. Finite-time consensus of heterogeneous multi-agent systems with and without velocity measurements. *Systems & Control Letters*, 61(8):871–878, 2012.